

Anomalous scaling of linear power corrections

Casey Farren-Colloty,^{1,*} Jack Helliwell,² Rtvik Patel,^{1,†} Gavin P. Salam,^{1,3} and Silvia Zanolini¹

¹*Rudolf Peierls Centre for Theoretical Physics, Clarendon Laboratory, Parks Road, Oxford OX1 3PU, UK*

²*School of Physics and Astronomy, Monash University, Wellington Rd, Clayton VIC-3800, Australia*

³*All Souls College, Oxford OX1 4AL, UK*

Non-perturbative corrections to hadronic observables represent a critical obstacle to increasing accuracy at colliders. Long taken to scale simply as $1/Q$, where Q is the centre-of-mass scattering energy, recent work has opened the path towards calculating the anomalous dimension that modifies that scaling. A priori, the problem is complex, requiring a resummation involving arbitrary numbers of large-angle and low-energy gluons. Within a specific framework for kinematic recoil, we show that it reduces to a simple exponential for key observables like the thrust, C -parameter and energy correlators. This simplicity holds for a specific hadron mass scheme, and also even beyond the two-jet limit.

The interpretation of ever more precise data from high-energy colliders requires corresponding improvements in the accuracy of theoretical predictions within the Standard Model (SM) of particle physics. One major avenue of progress involves advances [1, 2] in calculations using perturbative Quantum Chromodynamics (QCD). Yet, as perturbative accuracy increases, a second problem comes to the fore, namely that experiments measure non-perturbative hadrons rather than the quarks and gluons of perturbative QCD, and one must understand the relation between the two.

One powerful and widely used approach to this problem is to use phenomenological models to describe the transition from partons to hadrons, i.e. *hadronisation* [3–11]. However, such models bring little analytical insight into the problem and suffer from long-standing open questions about how to consistently combine them with the highest-accuracy perturbative calculations. An alternative approach exploits the renormalon breakdown of perturbation theory at high orders, a factorial growth in the perturbative coefficients [12], to gain insight into the potential structure of non-perturbative effects. This path offers the potential for greater understanding of the analytical structure of hadronisation.

The class of non-perturbative corrections that is largest numerically is that with a Λ/Q power scaling, where Λ is the non-perturbative scale of QCD and Q is the centre-of-mass energy. Such linear power corrections affect essentially all infrared safe observables that are based on hadron momenta. They were first explored in the mid-1990's [13–24] and are among the key elements that are extensively debated in determinations of the strong coupling constant from event shapes [25–30], with tensions of up to 3 standard deviations [27] relative to the world average [31].

One of the key results of the 1990's is that the renormalon approach reduces to probing how the emission of



FIG. 1. (a) emission of a non-perturbative *gluer* from a $q\bar{q}$ system, as in standard calculations; (b) a realistic set of perturbative partons from which a gluer would actually be emitted.

a single gluon at low transverse momentum modifies a given observable. That single gluon is sometimes referred to as a *gluer* [14]. This is illustrated in Fig. 1a, which shows the emission of a gluer (in red) in $e^+e^- \rightarrow q\bar{q}$ collisions.

Such an approach inevitably oversimplifies hadronisation, which seldom happens from a bare $q\bar{q}$ system, but instead almost always from a system where the $q\bar{q}$ has radiated multiple perturbative gluons, as in Fig. 1b. What long remained unclear, however, was how to extend the renormalon picture to systems with more than a $q\bar{q}$ pair. The past few years have started to see insight into this question [32–39] (for other recent hadronisation studies see e.g. Refs. [40–42]).

In the picture that is emerging, one can understand the effect of hadronisation by evaluating how an observable changes when inserting a gluer into each and every colour dipole of the event, using a well-chosen recoil scheme to account for momentum conservation.

Developing that picture for the thrust [43, 44] and C -parameter [45], Dasgupta and Hounat [46] have considered the average effect of gluer insertion, after integrating over the kinematics of a single perturbative soft gluon. They find that this leads to a modification of the coefficient of Λ/Q for the average value of those observables, observing a correction factor that involves an anomalous dimension, $1 - (\alpha_s/2\pi) C_A \mathcal{S}_1 \ln Q/\Lambda$, with $\mathcal{S}_1 \simeq 2.455$ common to both observables. As discussed there, the all-order resummation of the anomalous scaling would involve considering gluer emission from systems with arbitrary numbers of large-angle soft gluons, Fig. 1b. The goal of this letter is to carry out that resummation. A priori, one expects [46] to find a structure similar to that of non-global logarithms [47], for which no analytic re-

* Current address: Trinity College, Dublin 2, Ireland

† Current address: St. Catharine's College, Trumpington Street, Cambridge CB2 1RL, UK

summation result is known.

Starting from a $q\bar{q}$ system, the non-perturbative correction to an observable V can be written as

$$\langle \delta V_{\text{np}} \rangle_{q\bar{q}} = \int_0^{\mu_{\text{np}}} \frac{dk_{tn}}{k_{tn}} d\eta_n \frac{2C_F \alpha_s^{(\text{eff})}(k_{tn})}{\pi} \times [V(p_1, p_2, k_n) - V(\tilde{p}_1, \tilde{p}_2)], \quad (1)$$

where the p_i (\tilde{p}_i) are the hard momenta in the event after (before) emission of a soft non-perturbative gluon k_n . The integral is performed over its transverse momentum k_{tn} and rapidity η_n , weighted with $\alpha_s^{(\text{eff})}(k_{tn})$, an effective non-perturbative coupling for emitting the gluon at scales below an infrared matching scale $\mu_{\text{np}} \sim 1 \text{ GeV}$.

We consider observables V that are *linear*, i.e. reduce to linear functions of any number of soft massless momenta k_i emitted from the hard $q\bar{q}$ system

$$V(p_1, p_2, k_1 \dots, k_m) - V(\tilde{p}_1, \tilde{p}_2) = \sum_i \frac{k_{ti}}{Q} f_V(\eta_i) + \mathcal{O}\left(\frac{k_{ti}^2}{Q^2}\right), \quad (2)$$

specifically, the thrust (T , $f_T(\eta) = e^{-|\eta|}$, with $\tau \equiv 1 - T$), the C -parameter ($f_C(\eta) = 3/\cosh \eta$), and energy-energy correlators $\text{EEC}(\theta) = \sum_{ij} E_i E_j / Q^2 \delta(\theta_{ij} - \theta)$ [48, 49] ($f_{\text{EEC}}(\eta) = 2 \cosh^2 \eta \delta(\eta - \log(\tan \theta/2))$). Here k_{ti} and η_i are the transverse momentum and rapidity of i with respect to the $q\bar{q}$ pair. Eq. (1) then reduces to

$$\langle \delta V_{\text{np}} \rangle_{q\bar{q}} = c_V \frac{T_{q\bar{q}}}{Q}, \quad T_{q\bar{q}} = \int_0^{\mu_{\text{np}}} dk_{tn} \frac{2C_F \alpha_s^{(\text{eff})}(k_{tn})}{\pi}, \quad (3)$$

where $T_{q\bar{q}}$ can be interpreted as the effective non-perturbative transverse momentum produced per unit rapidity from a $q\bar{q}$ system, and $c_V = \int d\eta f_V(\eta)$, e.g. $c_T = 2$, $c_C = 3\pi$ and $c_{\text{EEC}(|\cos \theta| < 1/2)} = 4/\sqrt{3}$. The linearity of the observables ensures that the details of how that transverse momentum is produced, e.g. correlations between particles, do not matter.

The key question we ask here is how the transverse momentum per unit rapidity changes when the non-perturbative gluon emission takes place not from a $q\bar{q}$ pair, but from a system with arbitrary numbers of additional soft gluons, $qg_1 \dots g_m \bar{q}$. We will work in the large- N_c limit, considering gluon emission from a sequence of colour dipoles qg_1 , $g_1 g_2$, etc. The essential observation of Refs. [35, 36] is that for linear observables, the result of the renormalon calculation can be obtained using kinematic maps where the recoil of the hard partons is a linear function of the soft emitted gluon's momentum. It is important to be aware that this is yet to be proved for final-states with gluons, though the universality of soft emission suggests that the results should carry over.

We will consider two maps that satisfy the soft-gluon linearity condition: the 3-jet matched [50] Pan-Global [51, 52] and Pan-Local [51] maps. Both have the property that longitudinal recoil is local to the dipole. We have verified that our implementation reproduces the

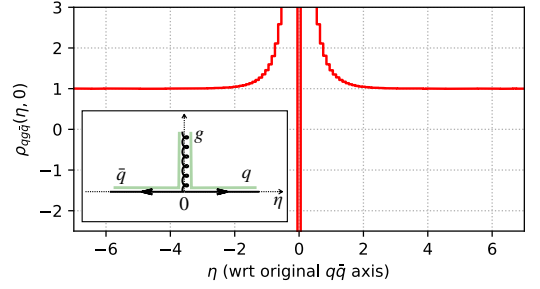


FIG. 2. The effect of gluon emission on transverse momentum per unit rapidity (η) in events consisting of a hard $q\bar{q}$ pair and a perturbative soft gluon at zero rapidity.

3-jet non-perturbative shifts of Refs. [25, 35, 36] (supplemental material [53], §1) and that the maps' predicted non-perturbative shifts for linear observables agree also for more complex dipole configurations, for sufficiently soft gluons.

We start by considering a gluon emission from $qg\bar{q}$ system, where the gluon itself is soft, and evaluate the non-perturbative transverse momentum per unit rapidity as a function of rapidity η relative to the $q\bar{q}$ system. That can be written as

$$T_{qg\bar{q}}(\eta, \eta_g) = \frac{C_A}{\pi} \sum_{qg, g\bar{q}} \int \frac{dz_+}{z_+} \frac{dk_{\perp n}}{k_{\perp n}} \frac{d\phi_n}{2\pi} [k_{tn} \delta(\eta - \eta_n) + (p_{tg} - \tilde{p}_{tg}) \delta(\eta - \eta_g)] \alpha_s^{(\text{eff})}(k_{\perp n}). \quad (4)$$

The square brackets contain the change in scalar transverse momentum (subscript t , with respect to the $q\bar{q}$ direction) due to the gluon emission n and recoil of the perturbative gluon g . The gluon integration variables $k_{\perp n}$ and z_+ are the transverse component and plus light-cone fraction defined with respect to the emitting qg or $g\bar{q}$ dipole. We neglect the transverse momenta of the q, \bar{q} , because they are at large rapidities, where $f_V(\eta)$ in Eq. (2) vanishes. Finally, the gluon must be much softer than the gluon. Rather than using some specific form for $\alpha_s^{(\text{eff})}(\mu)$, we probe how the observable changes on insertion of the gluon at a specific transverse momentum $k_{\perp n}$, then taking the limit of the gluon $k_{\perp n} \rightarrow 0$ [53], §1. Fig. 2 shows a numerical evaluation of

$$\rho_{qg\bar{q}}(\eta, \eta_g) \equiv T_{qg\bar{q}}(\eta, \eta_g) / T_{q\bar{q}} \quad (5)$$

for $\eta_g = 0$. At large rapidities, $\rho_{qg\bar{q}}(\eta, \eta_g)$ tends to 1 as expected from angular ordering. For η near zero, i.e. close to the perturbative gluon, a small $k_{\perp n}$ with respect to the qg or $g\bar{q}$ dipoles translates into a larger k_{tn} with respect to the $q\bar{q}$ direction, hence $\rho_{qg\bar{q}}(\eta) \gg 1$. Finally there is a negative δ -function at $\eta = \eta_g = 0$ associated with the $(p_{tg} - \tilde{p}_{tg})$ recoil of the perturbative gluon.

To obtain the logarithmically dominant contribution to Eq. (3) at NLO accuracy, we need to integrate $\rho_{qg\bar{q}}(\eta, \eta_g)$ over the perturbative soft gluon kinematics and account

for virtual corrections:

$$\mathcal{R}^{\text{NLO}} = 1 + \int d\eta_g \int_{\mu_{\text{np}}}^Q \frac{d\tilde{p}_{tg}}{\tilde{p}_{tg}} \frac{2C_F\alpha_s(\tilde{p}_{tg})}{\pi} [\rho_{qg\bar{q}}(\eta, \eta_g) - 1]. \quad (6)$$

This is the NLO factor that multiplies the average transverse momentum density. It is straightforward to show (Ref. [53], § 2) that

$$\int_{-\infty}^{+\infty} d\eta_g [\rho_{qg\bar{q}}(\eta, \eta_g) - 1] = -4(1 - \ln 2). \quad (7)$$

Replacing $2C_F \rightarrow C_A$ (large- N_c limit) yields,

$$\mathcal{R}^{\text{NLO}} = 1 - \lambda(Q, \mu_{\text{np}}) \frac{C_A \mathcal{S}_1}{2\pi}, \quad (8)$$

with

$$\mathcal{S}_1 = 8(1 - \ln 2), \quad \lambda(Q, \mu_{\text{np}}) = \int_{\mu_{\text{np}}}^Q \frac{dp_t}{p_t} \alpha_s(p_t), \quad (9)$$

in agreement with the numerical result of Ref. [46], but obtained generically for observables that are linear in the soft momenta and with $f(\eta) \rightarrow 0$ for large $|\eta|$.

Our approach can be straightforwardly extended to all orders. Specifically, let \mathcal{R} be a function of the hard scale Q , $\mathcal{R}(Q)$, such that $\mathcal{R}(\mu_{\text{np}}) = 1$. Given a certain $\mathcal{R}(Q)$, if we increase the hard scale by an infinitesimal factor $1 + \epsilon$, we allow for extra configurations with a soft gluon between scales Q and $(1 + \epsilon)Q$. Those extra configurations have a radiation pattern corresponding to dressed qg and $g\bar{q}$ dipoles, where the non-perturbative transverse momentum density with respect to the qg or $g\bar{q}$ dipole is $\mathcal{R}(Q)T_{q\bar{q}}$. Recall that we are using the large- N_c limit, thus the qg and $g\bar{q}$ dipoles have the same non-perturbative emission density as a $q\bar{q}$ dipole. This yields the following differential equation

$$\frac{d\mathcal{R}(Q)}{d\ln Q} = \frac{2C_F\alpha_s(Q)}{\pi} \int d\eta_g [\rho_{qg\bar{q}}(\eta, \eta_g) - 1] \mathcal{R}(Q), \quad (10)$$

where we make use of the property that the non-perturbative all-order longitudinal recoil from the qg or $g\bar{q}$ dipoles gets the same $\mathcal{R}(Q)$ factor as the transverse momentum density ([53], § 3). Once again using the large- N_c limit, $2C_F \rightarrow C_A$, the solution to Eq. (10) is

$$\mathcal{R}(Q) = \exp \left[-\lambda(Q, \mu_{\text{np}}) \frac{C_A \mathcal{S}_1}{2\pi} \right] = \left(\frac{\alpha_s(Q)}{\alpha_s(\mu)} \right)^{\frac{C_A \mathcal{S}_1}{\beta_0}}, \quad (11)$$

with $\beta_0 = (11C_A - 2n_f)/3$, such that Eq. (3) becomes

$$\langle \delta V_{\text{np}} \rangle = c_V \frac{T_{\text{all-order}}(Q)}{Q}, \quad T_{\text{all-order}}(Q) = T_{q\bar{q}} \mathcal{R}(Q). \quad (12)$$

This is much simpler than the structure one would expect from a non-global resummation, and part of the reason why such a structure emerges is the requirement of linearity of the observable in the soft limit, Eq. (2). The

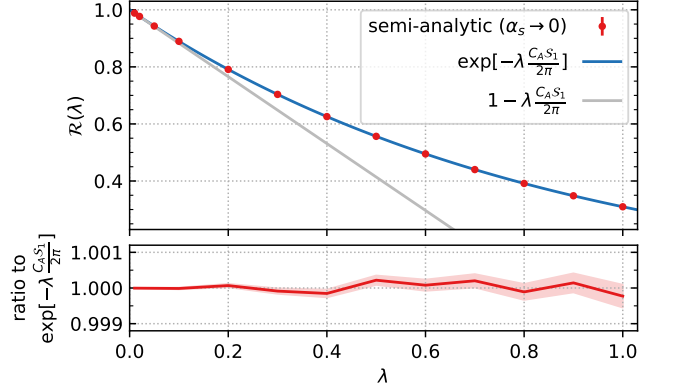


FIG. 3. All-order evaluation of \mathcal{R} , using a perturbative shower for the gluon cloud and a semi-analytic evaluation of the gluer insertion. The result is shown in the limit $\alpha_s \rightarrow 0$ at any given fixed λ , plotted as a function of λ and compared to the all-order analytic result, Eq. (11) (blue line).

exponentiated structure is important because there is a fundamental ambiguity in what scale one should take for μ_{np} , and Eq. (11) tells us that that ambiguity can simply be absorbed into the normalisation of $T_{q\bar{q}}$.

We supplement our analytic derivation with numerical tests. We start with a $q\bar{q}$ system, and use a perturbative parton shower [52, 54, 55] to add a cloud of soft gluons between scales $p_{t,\text{min}}$ and $p_{t,\text{max}} \ll Q$ (using fixed α_s for simplicity). We then have two ways of probing the gluer's effect. In one, we directly insert the gluer into the showered event. In the other, we use a semi-analytic calculation of the gluer's impact on the transverse momentum per unit rapidity for an arbitrary dipole [53], § 4 a. Fig. 3 shows results with the latter. We have run the shower in an asymptotic regime, $\alpha_s \rightarrow 0$ for fixed $\lambda = \alpha_s \ln p_{t,\text{max}}/p_{t,\text{min}}$, so as to extract just the $(\alpha_s \ln p_{t,\text{max}}/p_{t,\text{min}})^n$ terms, free of higher-logarithmic contamination. The results agree with Eq. (11) to within statistical errors, of order a few times 10^{-4} . The comparison to the pure first order result (grey line) illustrates the size of the resummation effect.

Our analysis has so far been for a $q\bar{q}$ event with a cloud of soft gluons, and since we integrate over all p_t values for the soft gluons, it is in effect inclusive over the value of the observable. Insofar as the linearity property of an observable holds beyond $q\bar{q}$ events, we would expect the same modification factor as in Eq. (11) to hold for the Λ/Q power correction also in the 3-jet limit. We test this by starting from 3-parton events, adding a cloud of soft gluons as done for Fig. 3, and then inserting gluers into all dipoles and determining the change in the value of the observable. Fig. 4 shows the resulting effective coefficient of the power correction to the C -parameter, $\delta C_{\text{np}}/[T_{q\bar{q}}/Q]$, as a function of the perturbative (3-parton) value of the C parameter. The red-dashed curve is without the cloud of soft gluons, the orange and cyan curves include the soft gluons. The lower panel shows the ratio to the plain

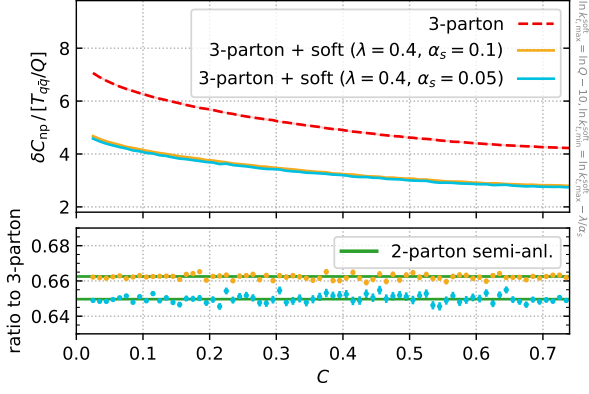


FIG. 4. The C -parameter non-perturbative correction in the 3-jet region, without (red) and with a cloud of soft gluons (orange, cyan). The lower panel shows that the ratio with and without soft gluons is independent of C and agrees with the corresponding 2-jet result at the same λ and α_s values (“2-parton semi-anl.”).

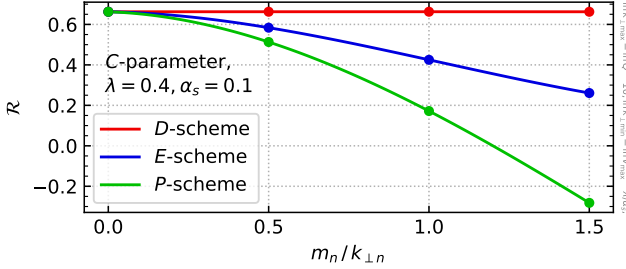


FIG. 5. Dependence of the scaling factor \mathcal{R} on the ratio of gluon mass to transverse momentum, in three difference hadron-mass schemes. Only in the decay (D) scheme are the results consistent with Eq. (11) also at non-zero gluon masses.

3-parton (no-cloud) result for two finite α_s values at fixed λ . The ratio coincides with the corresponding 2-jet result at the same λ and finite α_s values, slightly different from Eq. (11) because of subleading logarithmic effects present in the shower at finite α_s (“2-parton semi-anl.” [53], § 4b). This confirms that the universality of the anomalous dimension holds across the full spectrum. We find similar results for the thrust. Note that for small V , the 3-parton result itself goes as $c_V(1 - \frac{1}{2}\mathcal{S}_1/\ln \frac{1}{V})$, as required for consistency with the anomalous dimension [53] § 1 (see also Ref. [56]).

Fig. 4 uses a soft-gluon cloud with $p_{t,\max} \ll Q$. In practice, when the observable has a value $V \ll 1$, the actual $p_{t,\max}$ is limited to be $\lesssim \xi VQ$, with ξ of order 1. Thus we expect the shift to involve a factor $\mathcal{R}(\xi VQ)$ rather than $\mathcal{R}(Q)$, bringing additional V -dependence relative to the shape of the pure 3-parton result.

A further consideration is that hadrons have masses, while our analysis so far has been for massless gluon emission. There are various schemes for treating the hadron-mass dependence in the definitions of observables [57].

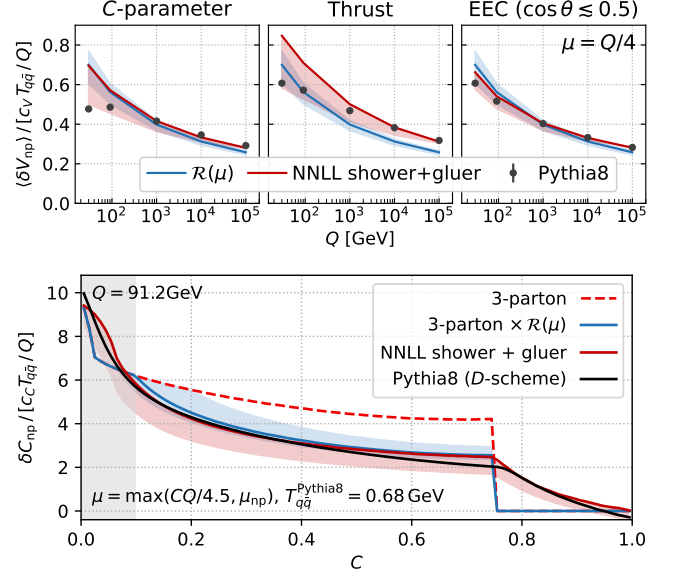


FIG. 6. Top: average C -parameter, τ and EEC, as a function of Q , comparing the $\mathcal{R}(\mu)$ calculation (Eq. (11)), gluon insertion into the NNLL PanGlobal shower, and Pythia8. For the EEC, $\lesssim 0.5$ indicates a continuous bin boundary [53], § 6. Bottom: the analogous set of results for the C -parameter distribution, with additionally the plain 3-parton result for comparison. In the grey area, we freeze μ in $\mathcal{R}(\mu)$ to $\mu_{np} = 2$ GeV.

Differences between schemes involve an anomalous scaling [57, 58] that differs from Eq. (11) and whose normalisation involves non-perturbative parameter(s) beyond $T_{q\bar{q}}$. We conjecture that one can probe the effect of hadron masses by examining the same class of shower kinematic maps with a *massive* gluon ([53], § 5). The results, Fig. 5, suggest one hadron-mass scheme is favoured, the D (or decay) scheme, where each hadron is isotropically decayed to two massless particles. In this scheme the anomalous dimension is universal, i.e. independent of the ratio of the gluon mass m_n to its transverse momentum $k_{\perp n}$. In other schemes, \mathcal{R} depends strongly on $m_n/k_{\perp n}$, implying that the hadronisation corrections depend on additional non-perturbative parameters beyond $T_{q\bar{q}}$, connected with the precise distribution of hadron masses and their transverse momenta.

We close with a comparison to hadronisation effects employing Pythia’s [59] widely used Lund string model [5, 6]. Exploring a range of Q values, Fig. 6 (top) shows the coefficient of the all-order non-perturbative correction to the average C -parameter, thrust and EEC results, specifically the ratio to the plain 2-parton expectation. The blue curve is Eq. (12) with $\mu_{np} = 2$ GeV, and the band covers $1/6 < \mu/Q < 1/2$. Our best prediction, the dark red curve, corresponds to the insertion of an asymptotically soft gluon, $k_{\perp n} \simeq 0.0015$ GeV, into actual showered events (NNLL PanGlobal [60] with a cutoff at μ_{np}). The light red band shows the effect of increasing $k_{\perp n}$ to 0.7 GeV, which gives a sense of the magnitude of

higher-power effects. These are surprisingly large even for $Q \sim 100$ GeV. The difference between the dark red and blue curves gives a measure of further higher-order perturbative effects.

The black points in Fig. 6 show the hadronisation corrections from Pythia 8.312 (Monash2013 tune [61]), using the D -scheme. To relate those to Eq. (12), we need to determine Pythia’s effective $T_{q\bar{q}}$, which we do by requiring agreement between the gluer insertion result and Pythia for the average C -parameter at $Q = 10^3$ GeV. This yields $T_{q\bar{q}}^{\text{Pythia}} = 0.68$ GeV. Across observables, there is good agreement between Pythia and our predicted scaling, notably at high Q values.

Finally, the lower panel of Fig. 6 shows the full C -parameter distribution at $Q = 91.2$ GeV, with the same set of curves as for the average, and additionally the pure 3-parton result for comparison (dashed-red). The agreement between our curves and Pythia is striking and one observes also a significant shape difference relative to the pure 3-parton result. This is connected with the dependence of the anomalous dimension’s scale on the C -parameter. For other energies, and the thrust (subject to larger subleading effects), see [53], § 7.

To summarise: our main result is the determination of the all-order structure of the anomalous scaling for the non-perturbative Λ/Q power correction to widely-studied linear observables like the thrust, C -parameter and energy correlators. This has been done within a paradigm where recoil from gluer insertion is linear in the gluer momentum [35, 36]. While the paradigm remains to be fully established, our results are sufficiently striking as to strongly motivate further study of its theoretical foundations. The most surprising finding is that despite the complicated structure of the soft-gluon cloud from which a non-perturbative gluer is emitted, the all-order result is a straightforward exponentiation, Eq. (11), of the first or-

der result [46]. This remains true even with a finite gluer mass, as long as one uses the D -scheme. Furthermore, this analytic approach reproduces the Q -dependence and event-shape dependence seen in Pythia, to within higher-order and higher-power effects that are larger than might have been expected from earlier studies. We look forward to future phenomenological applications of these insights.

ACKNOWLEDGMENTS

We are grateful to Fabrizio Caola for collaboration in the early stages of this work and one of us (GPS) wishes to acknowledge Pier Monni for some initial joint work on the all-order corrections to the C -parameter hadronisation. We thank Paolo Nason and Giulia Zanderighi for providing the code from Ref. [25] for the determination of the 3-parton power corrections. We are grateful also to Mrinal Dasgupta for sharing the results of Ref. [46] ahead of publication. We wish to thank all of the above, as well as Melissa van Beekveld and Silvia Ferrario Ravasio, for numerous discussions and helpful comments on the manuscript. We are grateful also to Andrea Banfi and Basem Kamal El-Menoufi for discussions during the final stages of this paper about a forthcoming result of theirs [56] that coincides with our Eq. (9) and with findings of our [53], § 1. This work has been funded by the European Research Council (ERC) under the European Union’s Horizon 2020 research and innovation programme (grant agreement No. 788223, JH, GPS, SZ), by a Royal Society Research Professorship (RP\R1\231001, CFC, RP, GPS), by the Science and Technology Facilities Council (STFC) under grants ST/T000864/1 (GPS), ST/X000761/1 (GPS, SZ) and by the Australian Research Council via Discovery Project DP220103512 (JH).

-
- [1] G. Heinrich, Phys. Rept. **922**, 1 (2021), arXiv:2009.00516 [hep-ph].
 - [2] J. M. Campbell *et al.*, in *Snowmass 2021* (2022) arXiv:2203.11110 [hep-ph].
 - [3] X. Artru and G. Mennessier, Nucl. Phys. B **70**, 93 (1974).
 - [4] M. G. Bowler, Z. Phys. C **11**, 169 (1981).
 - [5] B. Andersson, G. Gustafson, and B. Soderberg, Z. Phys. C **20**, 317 (1983).
 - [6] B. Andersson, G. Gustafson, G. Ingelman, and T. Sjostrand, Phys. Rept. **97**, 31 (1983).
 - [7] J. R. Christiansen and P. Z. Skands, JHEP **08**, 003, arXiv:1505.01681 [hep-ph].
 - [8] T. D. Gottschalk, Nucl. Phys. B **214**, 201 (1983).
 - [9] T. D. Gottschalk and D. A. Morris, Nucl. Phys. B **288**, 729 (1987).
 - [10] R. D. Field and S. Wolfram, Nucl. Phys. B **213**, 65 (1983).
 - [11] B. R. Webber, Nucl. Phys. B **238**, 492 (1984).
 - [12] M. Beneke, Phys. Rept. **317**, 1 (1999), arXiv:hep-ph/9807443.
 - [13] A. V. Manohar and M. B. Wise, Phys. Lett. B **344**, 407 (1995), arXiv:hep-ph/9406392.
 - [14] Y. L. Dokshitzer and B. R. Webber, Phys. Lett. B **352**, 451 (1995), arXiv:hep-ph/9504219.
 - [15] R. Akhouri and V. I. Zakharov, Phys. Lett. B **357**, 646 (1995), arXiv:hep-ph/9504248.
 - [16] P. Nason and M. H. Seymour, Nucl. Phys. B **454**, 291 (1995), arXiv:hep-ph/9506317.
 - [17] Y. L. Dokshitzer, G. Marchesini, and B. R. Webber, Nucl. Phys. B **469**, 93 (1996), arXiv:hep-ph/9512336.
 - [18] M. Beneke, V. M. Braun, and L. Magnea, Nucl. Phys. B **497**, 297 (1997), arXiv:hep-ph/9701309.
 - [19] Y. L. Dokshitzer and B. R. Webber, Phys. Lett. B **404**, 321 (1997), arXiv:hep-ph/9704298.
 - [20] Y. L. Dokshitzer, A. Lucenti, G. Marchesini, and G. P. Salam, Nucl. Phys. B **511**, 396 (1998), [Erratum: Nucl.Phys.B 593, 729–730 (2001)], arXiv:hep-ph/9707532.
 - [21] Y. L. Dokshitzer, A. Lucenti, G. Marchesini, and G. P. Salam, JHEP **05**, 003, arXiv:hep-ph/9802381.

- [22] M. Dasgupta and B. R. Webber, JHEP **10**, 001, arXiv:hep-ph/9809247.
- [23] M. Dasgupta, L. Magnea, and G. Smye, JHEP **11**, 025, arXiv:hep-ph/9911316.
- [24] G. P. Korchemsky and G. F. Sterman, Nucl. Phys. B **555**, 335 (1999), arXiv:hep-ph/9902341.
- [25] P. Nason and G. Zanderighi, JHEP **06**, 058, arXiv:2301.03607 [hep-ph].
- [26] G. Bell, C. Lee, Y. Makris, J. Talbert, and B. Yan, Phys. Rev. D **109**, 094008 (2024), arXiv:2311.03990 [hep-ph].
- [27] M. A. Benitez, A. H. Hoang, V. Mateu, I. W. Stewart, and G. Vita, On Determining $\alpha_s(m_Z)$ from Dijets in e^+e^- Thrust (2024), arXiv:2412.15164 [hep-ph].
- [28] P. Nason and G. Zanderighi, Fits of α_s from event-shapes in the three-jet region: extension to all energies (2025), arXiv:2501.18173 [hep-ph].
- [29] U. G. Aglietti, G. Ferrera, W.-L. Ju, and J. Miao, Phys. Rev. Lett. **134**, 251904 (2025), arXiv:2502.01570 [hep-ph].
- [30] M. A. Benitez, A. Bhattacharya, A. H. Hoang, V. Mateu, M. D. Schwartz, I. W. Stewart, and X. Zhang, A Precise Determination of α_s from the Heavy Jet Mass Distribution (2025), arXiv:2502.12253 [hep-ph].
- [31] S. Navas *et al.* (Particle Data Group), Phys. Rev. D **110**, 030001 (2024).
- [32] S. Ferrario Ravasio, P. Nason, and C. Oleari, JHEP **01**, 203, arXiv:1810.10931 [hep-ph].
- [33] S. Ferrario Ravasio, G. Limatola, and P. Nason, JHEP **06**, 018, arXiv:2011.14114 [hep-ph].
- [34] G. Luisoni, P. F. Monni, and G. P. Salam, Eur. Phys. J. C **81**, 158 (2021), arXiv:2012.00622 [hep-ph].
- [35] F. Caola, S. Ferrario Ravasio, G. Limatola, K. Melnikov, and P. Nason, JHEP **01**, 093, arXiv:2108.08897 [hep-ph].
- [36] F. Caola, S. Ferrario Ravasio, G. Limatola, K. Melnikov, P. Nason, and M. A. Ozelik, JHEP **12**, 062, arXiv:2204.02247 [hep-ph].
- [37] S. Makarov, K. Melnikov, P. Nason, and M. A. Ozelik, JHEP **05**, 153, arXiv:2302.02729 [hep-ph].
- [38] S. Makarov, K. Melnikov, P. Nason, and M. A. Ozelik, JHEP **01**, 074, arXiv:2308.05526 [hep-ph].
- [39] S. Makarov, K. Melnikov, P. Nason, and M. A. Ozelik, JHEP **11**, 112, arXiv:2408.00632 [hep-ph].
- [40] A. Banfi, B. K. El-Menoufi, and R. Wood, JHEP **08**, 221, arXiv:2303.01534 [hep-ph].
- [41] A. H. Hoang, O. L. Jin, S. Plätzer, and D. Samitz, JHEP **07**, 005, arXiv:2404.09856 [hep-ph].
- [42] H. Chen, P. F. Monni, Z. Xu, and H. X. Zhu, Phys. Rev. Lett. **133**, 231901 (2024), arXiv:2406.06668 [hep-ph].
- [43] S. Brandt, C. Peyrou, R. Sosnowski, and A. Wroblewski, Phys. Lett. **12**, 57 (1964).
- [44] E. Farhi, Phys. Rev. Lett. **39**, 1587 (1977).
- [45] R. K. Ellis, D. A. Ross, and A. E. Terrano, Nucl. Phys. B **178**, 421 (1981).
- [46] M. Dasgupta and F. Hounat, Exploring soft anomalous dimensions for $1/Q$ power corrections (2024), arXiv:2411.16867 [hep-ph].
- [47] M. Dasgupta and G. Salam, Phys. Lett. B **512**, 323 (2001), arXiv:hep-ph/0104277.
- [48] C. L. Basham, L. S. Brown, S. D. Ellis, and S. T. Love, Phys. Rev. Lett. **41**, 1585 (1978).
- [49] C. L. Basham, L. S. Brown, S. D. Ellis, and S. T. Love, Phys. Rev. D **17**, 2298 (1978).
- [50] K. Hamilton, A. Karlberg, G. P. Salam, L. Scyboz, and R. Verheyen, JHEP **03**, 224, arXiv:2301.09645 [hep-ph].
- [51] M. Dasgupta, F. A. Dreyer, K. Hamilton, P. F. Monni, G. P. Salam, and G. Soyez, Phys. Rev. Lett. **125**, 052002 (2020), arXiv:2002.11114 [hep-ph].
- [52] S. Ferrario Ravasio, K. Hamilton, A. Karlberg, G. P. Salam, L. Scyboz, and G. Soyez, Phys. Rev. Lett. **131**, 161906 (2023), arXiv:2307.11142 [hep-ph].
- [53] C. Farren-Colloty, J. Helliwell, R. Patel, G. P. Salam, and S. Zanolli, Supplemental material to this letter (2025).
- [54] M. van Beekveld *et al.*, SciPost Phys. Codeb. **2024**, 31 (2024), arXiv:2312.13275 [hep-ph].
- [55] M. van Beekveld, S. Ferrario Ravasio, J. Helliwell, A. Karlberg, G. P. Salam, L. Scyboz, A. Soto-Ontoso, G. Soyez, and S. Zanolli, Logarithmically-accurate and positive-definite NLO shower matching (2025), arXiv:2504.05377 [hep-ph].
- [56] A. Banfi and B. K. El-Menoufi (2025), presentation at Parton Showers and Resummation 2025.
- [57] G. P. Salam and D. Wicke, JHEP **05**, 061, arXiv:hep-ph/0102343.
- [58] V. Mateu, I. W. Stewart, and J. Thaler, Phys. Rev. D **87**, 014025 (2013), arXiv:1209.3781 [hep-ph].
- [59] C. Bierlich *et al.*, SciPost Phys. Codeb. **2022**, 8 (2022), arXiv:2203.11601 [hep-ph].
- [60] M. van Beekveld *et al.*, Phys. Rev. Lett. **134**, 011901 (2025), arXiv:2406.02661 [hep-ph].
- [61] P. Skands, S. Carrazza, and J. Rojo, Eur. Phys. J. C **74**, 3024 (2014), arXiv:1404.5630 [hep-ph].

SUPPLEMENTAL MATERIAL

1. Comparison of PanGlobal and PanLocal results to those in the literature

The core formula that we use when identifying the coefficient of the non-perturbative power correction with a given kinematic map is

$$\langle \delta V_{\text{np}} \rangle_{q\bar{q}} = \int_0^{\mu_{\text{np}}} \frac{dk_{tn}}{k_{tn}} d\eta_n \frac{2C_F \alpha_s^{(\text{eff})}(k_{tn})}{\pi} [V(p_1, p_2, k_n) - V(\tilde{p}_1, \tilde{p}_2)], \quad (13a)$$

$$= \frac{T_{q\bar{q}}}{Q} \lim_{\mu_0 \rightarrow 0} \int_0^{\mu_{\text{np}}} \frac{dk_{tn}}{k_{tn}} d\eta_n Q \delta(k_{tn} - \mu_0) \times [V(p_1, p_2, k_n) - V(\tilde{p}_1, \tilde{p}_2)] + \mathcal{O}\left(\frac{\Lambda^2}{Q^2}\right), \quad (13b)$$

where the linearity properties of the observable ensure that the limit is well defined.

In our study we employ the kinematic maps of two different parton showers, namely PanGlobal (PG) and PanLocal (PL), both with transverse-momentum ordering, i.e. $\beta_{\text{PS}} = 0$ in the language of Ref. [51].¹ The full details of the kinematic maps can be found in Appendix A of Ref. [55], however the essence is as follows. For a dipole ij , we define

$$\tilde{s}_{ij} = 2\tilde{p}_i \cdot \tilde{p}_j, \quad \tilde{s}_i = 2\tilde{p}_i \cdot Q, \quad \tilde{s}_j = 2\tilde{p}_j \cdot Q, \quad (14)$$

where Q is momentum of the e^+e^- system, and introduce

$$z_+ = k_{tn} \sqrt{\frac{\tilde{s}_j}{\tilde{s}_{ij}\tilde{s}_i}} e^{+\bar{\eta}_n}, \quad z_- = k_{tn} \sqrt{\frac{\tilde{s}_i}{\tilde{s}_{ij}\tilde{s}_j}} e^{-\bar{\eta}_n}. \quad (15)$$

For the PanGlobal map, we have

$$\bar{k}_n^\mu = r_L(z_+\tilde{p}_i^\mu + z_-\tilde{p}_j^\mu + k_{\perp n}^\mu), \quad (16a)$$

$$\bar{p}_i^\mu = r_L(1 - z_+)\tilde{p}_i^\mu, \quad (16b)$$

$$\bar{p}_j^\mu = r_L(1 - z_-)\tilde{p}_j^\mu, \quad (16c)$$

where k_n^μ is the momentum of the gluon, with $k_{\perp n}^2 = -(k_{tn})^2$. The gluon's transverse momentum with respect to the parent dipole, $|k_{\perp n}|$, satisfies $2z_+z_-\tilde{p}_i \cdot \tilde{p}_j = |k_{\perp n}|^2$. The rescaling factor r_L is chosen to ensure conservation of the squared 4-momentum of the system. All the event momenta then undergo a common boost to bring the event back to its original centre of mass. The details [52] of the rescaling and global boost only affect quadratic corrections.

For the PanLocal map, we have

$$k_n^\mu = z_+\tilde{p}_i^\mu + z_-\tilde{p}_j^\mu + k_{\perp n}^\mu, \quad (17a)$$

$$p_i^\mu = (1 - z_+)\tilde{p}_i^\mu + \frac{z_+z_-}{1 - z_+}\tilde{p}_j^\mu - k_{\perp n}^\mu, \quad (17b)$$

$$p_j^\mu = \frac{1 - z_+ - z_-}{1 - z_+}\tilde{p}_j^\mu, \quad (17c)$$

which explicitly conserves momentum, so no further boosts are required. The equations here are given for the case where i is the “splitter”, i.e. the parent dipole particle that absorbs the transverse component. In the PanLocal map, one chooses i to be the splitter with probability $f(\bar{\eta}_n)$ and j with probability $1 - f(\bar{\eta}_n)$, with $f(\bar{\eta})$ given by

$$f(\bar{\eta}) = \begin{cases} 0 & \text{if } \bar{\eta} < -1 \\ \frac{15}{16} \left(\frac{\bar{\eta}^5}{5} - \frac{2\bar{\eta}^3}{3} + \bar{\eta} + \frac{8}{15} \right) & \text{if } -1 \leq \bar{\eta} \leq 1 \\ 1 & \text{if } \bar{\eta} > 1 \end{cases}. \quad (18)$$

Based on the discussion in Refs. [35, 36], both of these maps are expected to be suitable for determining the coefficient of the linear power correction, with the critical element being the continuity in the treatment of the recoil momenta

¹ Given that the PanLocal shower requires $0 < \beta_{\text{PS}} < 1$ for logarithmic accuracy, it may seem surprising that we use it here with $\beta_{\text{PS}} = 0$. The point is that we are probing the effect of a gluon insertion with an asymptotically soft gluon, $\mu_0 \rightarrow 0$. Thus, the choice of the ordering variable makes no difference when probing the effect of the soft gluon, because that soft gluon will always come as the last step regardless of β_{PS} . Note that for linear observables, the transverse recoil contributions, which would cause problems with logarithmic accuracy with $\beta_{\text{PS}} = 0$, simply average to zero after azimuthal integration when evaluating gluon insertion effects.

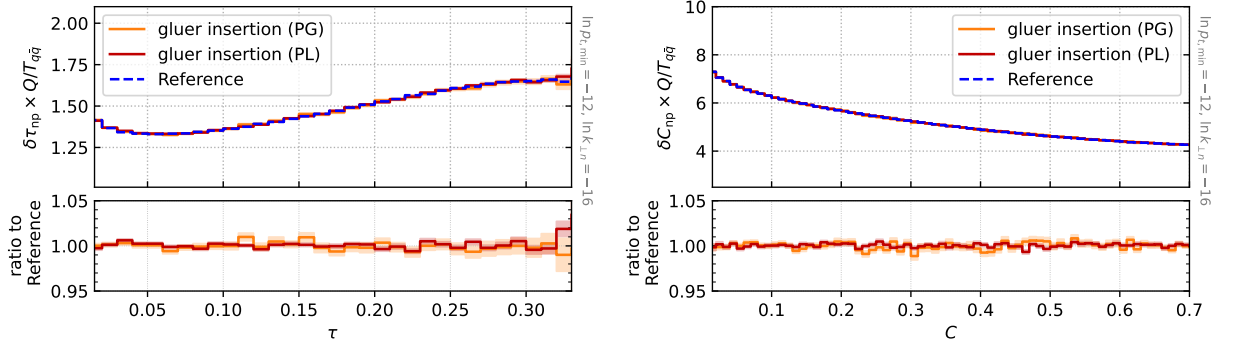


FIG. 7. Average non-perturbative shift for thrust (left) and C -parameter (right) for 3-parton configurations. Results are obtained for PanGlobal (orange, solid) and PanLocal (dark red, solid), and compared to the Reference results of [35, 36] as embodied in the code provided by the authors of Ref. [25] (blue, dashed), in the large- N_c limit.

as a function of $\bar{\eta}_n$. One should be aware that there remain open questions as to the validity of this general approach when one of the dipole ends is a gluon. In the large- N_c limit, given that we are considering just soft physics, one could make the argument that it is plausible that gluons and quarks should be treated similarly. Existing results in Refs. [25, 28, 35, 36] also use such an assumption. A further point to keep in mind is that we consider the emission of just a single soft on-shell gluer, rather than an off-shell gluer that splits to a gluon pair or $q\bar{q}$ pair. For observables linear in the soft limit, such as those that we consider here, the single on-shell gluer approach reproduces the structure of a full off-shell approach to within a universal “Milan-factor” constant [20–23].

We now show that our approach correctly reproduces results already available in the literature. We start by calculating the leading non-perturbative power correction for 3-parton configurations, and comparing to the results of [35, 36] as embodied in the code provided by the authors of Ref. [25]. We generate a $q\bar{q}g$ event using both PG and PL as tree-level generator, and we include the correct $q\bar{q}g$ matrix element using the multiplicative matching of Ref. [50]. The gluon transverse momentum p_{tg} is constrained to be larger than the shower cutoff $p_{t,\min}$, $p_{tg} > p_{t,\min}$. Given this constraint, the kinematics of the perturbative gluon is sampled randomly by the parton shower. Starting from this 3-parton configuration, a non-perturbative gluer is emitted with a transverse momentum $k_{\perp n}$ much smaller than the shower cutoff, $k_{\perp n} \ll p_{t,\min}$.

Our results are obtained in the large- N_c limit, as standard for dipole showers, while Refs. [25, 35, 36] perform the calculation in full colour. In order to perform this comparison, we thus extract the large- N_c limit of Ref. [25] considering only contributions from the qg and $\bar{q}g$ dipoles, which are proportional to $C_A/2$, and neglecting the $q\bar{q}$ dipole, as it would generate terms proportional to $C_F - C_A/2$, which vanish in the limit we are considering. Fig. 7 shows the leading non-perturbative shift in a 3-jet configuration for the thrust (left) and the C -parameter (right) as obtained with PanGlobal and PanLocal, compared to Refs. [25, 35, 36] (“Reference”). In both cases we find agreement with the reference results.

We conclude this section by reproducing the value of the anomalous dimension \mathcal{S}_1 through a numerical study of the behaviour of the non-perturbative power correction in the approach to the 2-jet limit. In particular, we connect to the result of [46], where \mathcal{S}_1 has been obtained in a semi-analytic way for the thrust and the C -parameter. We generate a $q\bar{q}$ event and emit a soft perturbative gluon at a scale higher than the shower cutoff, $k_{tg} > k_{t,\min}$. The differential weight associated to this configuration is $d\sigma$. The non-perturbative correction is then probed through the emission of a very soft gluer, $k_{tn} \ll k_{t,\min}$.

The average non-perturbative shift to an event-shape V at NLO accuracy is obtained as

$$\langle \delta V \rangle_{\text{np}}^{\text{NLO}} = \int d\ln V \frac{d\langle \delta V \rangle_{\text{np}}^{\text{NLO}}}{d\ln V} = \int d\ln V (\langle \delta V \rangle_{\text{np}} - \langle \delta V \rangle_{\text{np}}^{\text{Born}}) \frac{1}{\sigma} \frac{d\sigma}{d\ln V}, \quad (19)$$

where the term in brackets represents the difference between the average non-perturbative shift in a 3-parton configuration ($q\bar{q}g$) and in a Born ($q\bar{q}$) configuration. This expression has been obtained as follows: at NLO accuracy, we need to consider $\mathcal{O}(\alpha_s)$ corrections associated with the emission of a perturbative gluon g from a $q\bar{q}$ system. When considering the leading anomalous dimension \mathcal{S}_1 , we work in the asymptotic region, where real and virtual corrections are equal but with opposite sign. Real and virtual corrections are summed together: when integrating over the gluer insertion, we obtain the term in brackets, which is the difference of the contribution given by a gluer insertion in a $q\bar{q}g$ event (real correction) and in a $q\bar{q}$ event (virtual correction). This expression is reweighted by the probability of emitting a soft perturbative gluon $d\sigma$, which is obtained integrating over the gluon kinematics. Note that the term in

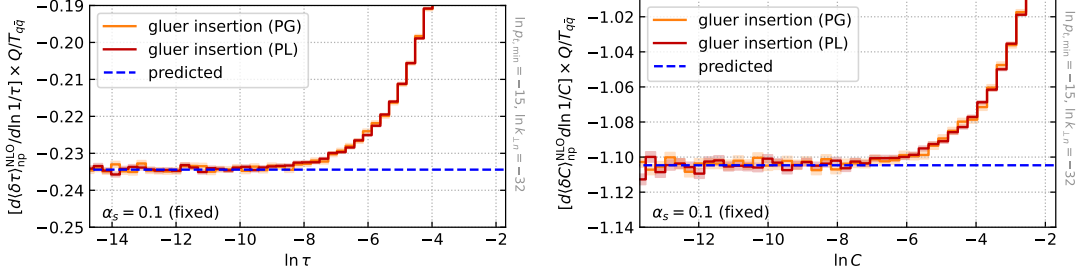


FIG. 8. Approach to the 2-jet limit for thrust (left) and C -parameter (right), showing the integrand of Eq. (19). Results are given for the PanGlobal (orange, solid) and PanLocal (dark red, solid) maps. The predicted value (blue, dotted) corresponds to $-c_V \frac{C_A \alpha_s}{2\pi} \mathcal{S}_1$.

brackets is expected to have an inverse logarithmic scaling in the event shape V which is governed by the anomalous dimension \mathcal{S}_1 :

$$\langle \delta V \rangle_{\text{np}} - \langle \delta V \rangle_{\text{np}}^{\text{Born}} = -\frac{C_A}{4C_F} \frac{\mathcal{S}_1}{(\ln d_V/V) - 3/4} \frac{c_V T_{q\bar{q}}}{Q}, \quad |\ln V| \gg 1, \quad \begin{cases} d_C = 6 \\ d_\tau = 1 \end{cases}. \quad (20)$$

The potential presence of a $1/\ln V$ structure had already been noted in Ref. [25]. The inverse logarithmic scaling arises because it is only when the perturbative gluon is at central rapidities that $\langle \delta V \rangle_{\text{np}}$ differs substantially from $\langle \delta V \rangle_{\text{np}}^{\text{Born}}$, cf. Fig. 2. That the normalisation should be as written is a consequence of the following argument. When approaching the 2-jet limit ($V \ll 1$), the perturbative distributions for the thrust and C -parameter have a well-known logarithmic enhancement

$$\frac{1}{\sigma} \frac{d\sigma}{d \ln 1/V} = \frac{2\alpha_s C_F}{\pi} \left(\ln \frac{d_V}{V} - \frac{3}{4} \right), \quad |\ln V| \gg 1. \quad (21)$$

Thus the integrand in Eq. (19) is free of logarithms and tends to a constant for large $|\ln V|$. The integral must reproduce the anomalous dimension shown in the text, i.e. the integrand must tend to $-c_V \frac{C_A \alpha_s}{2\pi} \mathcal{S}_1 \cdot T_{q\bar{q}}/Q$, and this tells us the expected normalisation in Eq. (20).

Figure 8 shows the numerically approach of the integrand to the 2-jet limit for the thrust (left) and the C -parameter (right), using the PanGlobal (orange, solid) and PanLocal (dark red, solid) maps for gluer insertion. In both cases, as $|\ln V|$ becomes large, the results tend to a plateau, which is agreement with the predicted value.

2. Analytic derivation of \mathcal{S}_1

The essence of our derivation will be to consider an observable that is the sum of transverse momenta inside a rapidity window $|\eta| < Y$ with $Y \gg 1$

$$S_t(Y) = \sum_i p_{ti} \Theta(|\eta_i| < Y), \quad (22)$$

where the p_i in this definition are to be understood as running over all momenta, whether perturbative or non-perturbative. One may define the p_{ti} to be the transverse component with respect to the thrust axis or with respect to some specific jet-axis definition for each of two exclusive jets. We will consider Y to be large but not so large that it includes the q or \bar{q} .

The key quantity that we want to calculate is the change in $S_t(Y)$ due to gluer emission. In a $q\bar{q}$ event, this is simply given by

$$\langle \delta S_t(Y) \rangle_{q\bar{q}} = 2Y T_{q\bar{q}}. \quad (23)$$

Next, we consider a $qg\bar{q}$ event, where a soft perturbative gluon g has been emitted at rapidity $\eta_g = 0$. Aligning the $q\bar{q}$ system along the z -direction, the gluon 4-momentum (p_x, p_y, p_z, E) is

$$\tilde{p}_g = \tilde{p}_{tg}(0, 1, 0, 1), \quad (24)$$

where the transverse momentum with respect to the $q\bar{q}$ axis (\tilde{p}_{tg}) is much smaller than the hard scale Q , $\tilde{p}_{t,g} \ll Q$. We now insert a non-perturbative gluer into the event. We focus first on the $\bar{q}g$ dipole (where the \bar{q} has negative p_z) and apply the map in Eq. (16) with $i = g$, $j = \bar{q}$ ($p_{\bar{q}z} < 0$). After application of the map, the momenta of interest are those that are potentially inside the rapidity window, i.e. p_g and k_n (using $r_L \rightarrow 1$),

$$p_g = (1 - z_+) \tilde{p}_{tg} (0, 1, 0, 1), \quad (25a)$$

$$k_n = \left(k_{\perp n} \sin \phi_n, \tilde{p}_{tg} z_+ + k_{\perp n} \cos \phi_n, -\frac{k_{\perp n}^2}{2\tilde{p}_{tg} z_+} - k_{\perp n} \cos \phi_n, \frac{k_{\perp n}^2}{2\tilde{p}_{tg} z_+} + \tilde{p}_{tg} z_+ + k_{\perp n} \cos \phi_n \right). \quad (25b)$$

The perturbative gluon itself will always be in the window. To determine whether the non-perturbative gluer will be in the window, we consider the limit $z_+ \ll k_{\perp n} / \tilde{p}_{tg}$, where we obtain

$$\eta_n = -\log \frac{k_{\perp n}}{\tilde{p}_{tg} z_+} > -Y \quad \rightarrow \quad z_+ > \frac{k_{\perp n}}{\tilde{p}_{tg}} e^{-Y}. \quad (26)$$

Thus we have

$$\delta S_t(Y) = -\tilde{p}_{tg} z_+ + \sqrt{k_{\perp n}^2 + \tilde{p}_{tg}^2 z_+^2 + 2z_+ \tilde{p}_{tg} k_{\perp n} \cos \phi} \Theta \left(z_+ > \frac{k_{\perp n}}{\tilde{p}_{tg}} e^{-Y} \right). \quad (27)$$

The integral over the gluer kinematics so as to obtain the average shift can be written as

$$\langle \delta S_t(Y) \rangle_{\bar{q}g} = T_{q\bar{q}} \lim_{k_{\perp n} \rightarrow 0} \left[\frac{1}{k_{\perp n}} \int_0^{2\pi} \frac{d\phi}{2\pi} \int_{\frac{k_{\perp n}}{\tilde{p}_{tg}} e^{-Y}}^1 \frac{dz_+}{z_+} \delta S_t(Y) \right]. \quad (28)$$

For the time being we work in the large- N_C limit, so that the $\bar{q}g$ dipole has the same colour factor as the $q\bar{q}$ dipole, allowing us to reuse $T_{q\bar{q}}$. Additionally, in setting the lower limit on the z_+ integral, we have exploited the fact that the $-\tilde{p}_{tg} z_+$ term in Eq. (27) contributes negligibly for z_+ values below the limit, yielding a term suppressed by a power of e^{-Y} , which we can omit. To evaluate Eq. (28) we first carry out the z_+ integration,

$$\frac{\langle \delta S_t(Y) \rangle_{\bar{q}g}}{T_{q\bar{q}}} = \lim_{k_{\perp n} \rightarrow 0} \int_0^{2\pi} \frac{d\phi}{2\pi} \left[F(z_+, \phi) \right]_{z_+ = \frac{k_{\perp n}}{\tilde{p}_{tg}} e^{-Y}}^{z_+ = 1} \quad (29)$$

with

$$F(z_+, \phi) = \frac{\sqrt{\tilde{p}_{tg}^2 z_+^2 + 2\tilde{p}_{tg} k_{\perp n} z_+ \cos(\phi) + k_{\perp n}^2}}{k_{\perp n}} - \frac{\tilde{p}_{tg} z_+}{k_{\perp n}} - \tanh^{-1} \left(\frac{\tilde{p}_{tg} z_+ \cos(\phi) + k_{\perp n}}{\sqrt{\tilde{p}_{tg}^2 z_+^2 + 2\tilde{p}_{tg} k_{\perp n} z_+ \cos(\phi) + k_{\perp n}^2}} \right) + \cos(\phi) \tanh^{-1} \left(\frac{\tilde{p}_{tg} z_+ + k_{\perp n} \cos(\phi)}{\sqrt{\tilde{p}_{tg}^2 z_+^2 + 2\tilde{p}_{tg} k_{\perp n} z_+ \cos(\phi) + k_{\perp n}^2}} \right). \quad (30)$$

With some manipulation, one can show that

$$F(1, \phi) + F(1, \phi + \pi) = \mathcal{O} \left(\frac{k_{\perp n}}{\tilde{p}_{tg}} \right), \quad (31)$$

such that the upper z_+ limit in Eq. (29) vanishes. As concerns the lower limit, one can show that

$$F \left(\frac{k_{\perp n}}{\tilde{p}_{tg}} e^{-Y}, \phi \right) = -Y - \frac{1}{2} \log(4 \csc^2 \phi) - \frac{1}{2} \cos(\phi) \log \left(\tan^2 \frac{\phi}{2} \right) + 1 + \mathcal{O}(e^{-Y}). \quad (32)$$

Taking the limit of large Y and small $k_{\perp n} / \tilde{p}_{tg}$, one can then carry out the ϕ integration, obtaining

$$\frac{\langle \delta S_t(Y) \rangle_{\bar{q}g}}{T_{q\bar{q}}} = Y - 2(1 - \log 2). \quad (33)$$

Taking into account the second (gq) dipole and evaluating the difference between the $\bar{q}g + gq$ and the $\bar{q}q$ contributions to $\delta S_t(Y)$ gives us

$$\langle \delta S_t(Y) \rangle_{\bar{q}g} + \langle \delta S_t(Y) \rangle_{gq} - \langle \delta S_t(Y) \rangle_{\bar{q}q} = -4(1 - \log 2) T_{q\bar{q}} \quad (34)$$

which corresponds to the result given in Eq. (7), but derived bypassing the intermediate $\rho_{qg\bar{q}}(\eta, \eta_g)$ quantity, which would have been more complicated to handle analytically.

We close this section with a brief comment on the subleading-colour contributions. At full colour, there would be a $C_A/(2C_F)$ factor in $\langle \delta S_t(Y) \rangle_{\bar{q}q}$ and $\langle \delta S_t(Y) \rangle_{gq}$, and an additional $(2C_F - C_A)/(2C_F) \langle \delta S_t(Y) \rangle_{\bar{q}q}$ dipole contribution. Taken together this would give an overall $C_A/2C_F$ factor in the full-colour equivalent of Eq. (34). That $C_A/2C_F$ factor would multiply the C_F factor in Eq. (6) ultimately giving us the C_A factor as in Eq. (8).

3. Universality of longitudinal recoil

The observables that we consider in the main text all have the property that $f_V(\eta)$ in Eq. (2) vanishes for large soft-particle rapidities η_i , so that for a $q\bar{q}$ system longitudinal recoil of the q and \bar{q} does not affect the observable. However, as soon as we have a perturbative gluon at large angles, emission of a gluon from a qg dipole will induce longitudinal recoil of the perturbative gluon, where longitudinal is now defined with respect to the qg dipole directions. Since the perturbative gluon is at large angles, this will affect the observable. A key assumption that underlies our derivation of Eq. (10) is that if we have a perturbative $qg\bar{q}$ system, then in any small patch of phase space that contains the perturbative gluon, the all-order resummation for the power correction to the energy flow in the patch will have the same correction factor as a patch without a gluon. The purpose of this section is to provide an understanding of why this condition is true.

The route that we take to establish this point is to start with a $q\bar{q}$ system. We will demonstrate that the corrections to energy flow in a patch containing the quark or anti-quark acquire the same first order correction as a patch not containing either. Once this is established, then for a $qg\bar{q}$ system the same argument will hold as concerns energy flow in a patch containing the g end of each of the qg and $g\bar{q}$ dipoles with respect to emission of a further gluon from each of those dipoles. Recursively applying this argument gives the all-order demonstration of the property that we need.

We start with a $q\bar{q}$ system and consider the light-cone plus component at rapidities larger than Y

$$S_+(Y) = \sum_i p_{+i} \Theta(\eta_i > Y), \quad (35)$$

where $p_{+i} = E_i + p_{zi}$ and the sum includes the q and \bar{q} if they are in the rapidity region (as in Eq. (22), the p_i run over all momenta, whether perturbative or non-perturbative). One way of analysing the observable is to note that if we take the limit $Y \rightarrow -\infty$, then $S_+(-\infty) = Q$, since all the z components cancel and the sum of energy components must add up to the centre-of-mass energy. Thus $S_+(-\infty)$ has no power correction, i.e. $\langle \delta S_+(-\infty) \rangle_{\bar{q}q} = 0$. Therefore we can express $\langle \delta S_+(Y) \rangle$ by considering the difference between $S_+(Y)$ and $S_+(-\infty)$, which involves a convergent integral over rapidities,

$$\langle \delta S_+(Y) \rangle_{q\bar{q}} = \langle \delta S_+(-\infty) \rangle_{q\bar{q}} - T_{q\bar{q}} \int_{-\infty}^Y d\eta e^\eta = -T_{q\bar{q}} e^Y. \quad (36)$$

Next, we consider a system with a soft perturbative gluon. For a specific soft-gluon rapidity η_g , the impact of the gluon on transverse momentum flow has a strong dependence on the rapidity, cf. Fig. 2. Similarly the impact of the gluon on $S_+(Y)$ will depend strongly on which dipole we consider and whether the perturbative gluon has rapidity larger or smaller than Y (e.g. if the $\eta_g \ll Y$ and one considers the qg dipole with the quark having positive p_z , then $\delta S_+(Y)_{qg}$ will be the same as $\delta S_+(Y)_{q\bar{q}}$, while $\delta S_+(Y)_{\bar{q}g}$ will be zero). However, once we integrate over the rapidity of the perturbative soft gluon, the impact of the gluon on the transverse momentum per unit rapidity will be independent of rapidity. Let us label the net non-perturbative transverse momentum per unit rapidity, after integrating over the perturbative gluon, as $T_{qg\bar{q}}$. Since $S_+(-\infty)$ always has the property that its non-perturbative change is zero, we can follow the same logic as used in Eq. (36) to obtain

$$\langle \delta S_+(Y) \rangle_{qg\bar{q}} = -T_{qg\bar{q}} e^Y. \quad (37)$$

This same argument can be applied to any order as long as the effect of the gluon, after averaging over perturbative emissions, remains independent of rapidity.

As a further verification, we also carried out an explicit numerical study. Rather than a sharp boundary $\Theta(\eta_i > Y)$, numerically it is more stable to use a boundary with a continuous turn-on, cf. also §6. Specifically, we include a particle's plus component with a weight $f_{0\pm\frac{1}{2}}(\eta)$ corresponding to a continuous turn on between $\eta = -\frac{1}{2}$ and $+\frac{1}{2}$

$$\tilde{S}_+ = \sum_i p_{+i} f_{0\pm\frac{1}{2}}(\eta_i), \quad f_{0\pm\frac{1}{2}}(\eta) = \Theta\left(-\frac{1}{2} < \eta < \frac{1}{2}\right) \left(\eta + \frac{1}{2}\right) + \Theta\left(\eta \geq \frac{1}{2}\right). \quad (38)$$

We then look at how \tilde{S}_+ changes when integrating over all possible gluer insertions. For a $q\bar{q}$ system, it is straightforward to show that this leads to the relation

$$\langle \delta \tilde{S}_+ \rangle_{q\bar{q}} = -\frac{e-1}{\sqrt{e}} T_{q\bar{q}} \simeq -1.04219 T_{q\bar{q}}. \quad (39)$$

We then verified this numerically in both a $q\bar{q}$ system and in $qg\bar{q}$ systems, where in the latter we integrate over the rapidity of the soft gluon g , with $p_{tg}/Q \simeq e^{-10}$, giving

$$\langle \delta \tilde{S}_+ \rangle_{q\bar{q}} / T_{q\bar{q}} = -1.04211 \pm 0.00055, \quad (40a)$$

$$\langle \delta \tilde{S}_+ \rangle_{qg\bar{q}} / T_{qg\bar{q}} = -1.04174 \pm 0.00082, \quad (40b)$$

both in good agreement with Eq. (39). Thus we see that the relation between average transverse and longitudinal gluer-induced shifts is preserved in systems with a soft gluon. It is enough to have verified this for a single smooth boundary to know that the relation will hold for arbitrary patches, because the relation between any two patches (smooth or not) only involves an integral over a finite range of rapidities, where only the emitted transverse component contributes, not the longitudinal recoil along the $q\bar{q}$ direction.

4. Numerical evaluation of \mathcal{R}

Given the surprising simplicity of Eq. (11), it is important to verify it numerically. To do so, we start with a $q\bar{q}$ system, and use a perturbative parton shower to add a cloud of soft gluons between scales $p_{t,\min}$ and $p_{t,\max} \ll Q$. Summing over all the perturbative dipoles, we then probe the effect of adding a much softer gluer at a single scale $k_{\perp n} \ll p_{t,\min}$. As an observable we use the transverse momentum in a central rapidity bin with respect to the $q\bar{q}$ direction. For the shower itself, we use the transverse momentum-ordered PanGlobal shower [52] of the PanScales code [54], version 0.3, in its split-dipole-frame, $\beta = 0$ variant, $\text{PG}_{\beta=0}^{\text{sdf}}$.

We have two approaches to probe the effect of the gluer: direct insertion together with a limit as in Eq. (13b), and a semi-analytic approach, § 4 a. With the choice of $\text{PG}_{\beta=0}^{\text{sdf}}$ for the perturbative shower, multiple soft-gluon production is invariant under longitudinal boosts along the $q\bar{q}$ axis, a property that helps ensure that when the perturbative shower is used with finite α_s values, subleading corrections are identical between the two gluer insertion approaches, as we will confirm below in § 4 b.

a. Semi-analytic approach

In the semi-analytic approach used for Fig. 3, we aim to determine the effect of gluer emission on the transverse momentum per unity rapidity, i.e. observables akin to $S_t(Y)$, Eq. (22). In the main text, we showed $\rho_{qg\bar{q}}(\eta, \eta_g)$ for a $qg\bar{q}$ system (Fig. 2), but ultimately only needed its integral over η_g , Eq. (7). We can apply an analogous strategy for more complex system. Specifically, we consider a generic dipole ij and use an approach similar to that of § 2 to determine an analytic function that can be integrated with adaptive Gaussian integration and that is equivalent to

$$I_{ij}(\Delta\eta_{ij}, \Delta\phi_{ij}) = \int_{-\infty}^{+\infty} d\eta_n \rho_{ij}(\eta_n, \eta_i, \eta_j, \Delta\phi_{ij}), \quad (41)$$

where $\rho_{ij}(\eta_n, \eta_i, \eta_j, \Delta\phi_{ij})$ is the analogue of $\rho_{qg\bar{q}}(\eta, \eta_g)$ but now for the ij dipole (with the ϕ_n dependence already integrated). We then tabulate I_{ij} as a function of $\Delta\eta_{ij}$ and $\Delta\phi_{ij}$, with the result shown in Fig. 9. Note that at large $\Delta\eta_{ij}$ separations, $I_{ij}(\Delta\eta_{ij}, \Delta\phi_{ij})$ tends to $\Delta\eta_{ij} - \frac{1}{2}\mathcal{S}_1$, independently of $\Delta\phi_{ij}$, because the neighbourhood of i is unaffected by the specific location of j , and so the analysis of § 2 becomes valid. For small ij separations $I_{ij}(\Delta\eta_{ij}, \Delta\phi_{ij})$ tends to zero, as is required for compatibility with the fact that a collimated ij dipole emits little soft radiation.

Because of the longitudinal boost invariance of the configurations of the perturbative soft gluon cloud, dipoles are uniformly distributed in rapidity along the $q\bar{q}$ direction. As a result, when determining the effect of gluer emission on the transverse momentum flow at a given rapidity, it is only the integral of $\rho_{ij}(\eta, \eta_i, \eta_j, \Delta\phi_{ij})$ over the dipole rapidity, $(\eta_i + \eta_j)/2$, that matters. Accordingly, we are free to replace $\rho_{ij}(\eta, \eta_i, \eta_j, \Delta\phi_{ij})$ with any function that yields the same integral when integrating over $(\eta_i + \eta_j)/2$. We take the specific form

$$\rho_{ij}(\eta, \eta_i, \eta_j, \Delta\phi_{ij}) \rightarrow \bar{\rho}_{ij}(\eta, \eta_i, \eta_j, \Delta\phi_{ij}) = \Theta(\eta_i < \eta < \eta_j) + \frac{1}{2} [\delta(\eta - \eta_i) + \delta(\eta - \eta_j)] [I_{ij}(\Delta\eta_{ij}, \Delta\phi_{ij}) - \Delta\eta_{ij}] \quad (42)$$

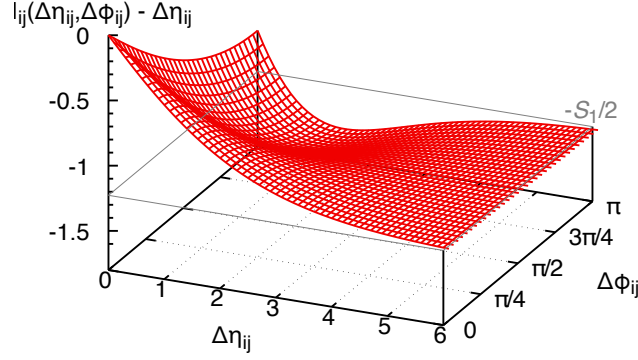


FIG. 9. 2d grid of $I_{ij}(\Delta\eta_{ij}, \Delta\phi_{ij})$, with $\Delta\eta_{ij}$ subtracted to as to better visualise the asymptotic behaviour, where the result (after subtraction) tends to $-S_1/2$, shown as the grey plane outline.

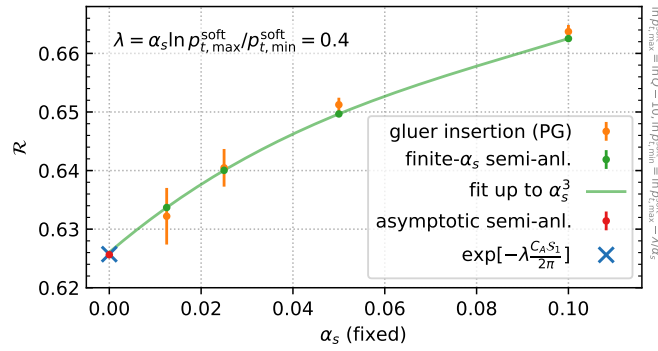


FIG. 10. Numerical all-order results for \mathcal{R} where the perturbative soft gluon cloud has been produced at several finite (fixed) α_s values and a transverse momentum range $\ln p_{t,\max}^{\text{soft}}/Q = -10$ down to $\ln p_{t,\max}^{\text{soft}}/Q = -10 - 0.4/\alpha_s$, as well as at asymptotically small α_s in the semi-analytic approach.

For a qi dipole with a quark along the positive z axis we take

$$\rho_{qi}(\eta, \eta_i,) \rightarrow \bar{\rho}_{qi}(\eta, \eta_i) = \Theta(\eta > \eta_i) - \frac{1}{4} S_1 \delta(\eta - \eta_i), \quad (43)$$

and analogously for a $\bar{q}i$ along the negative z axis.

To obtain the semi-analytic results in Figs. 10 and 3, we then sample over configurations of perturbative soft-gluon clouds and then determine the following average

$$\langle \delta S_t(Y) \rangle = T_{q\bar{q}} \left\langle \sum_{ij \in \text{dipoles}} \int_{-Y}^Y d\eta \bar{\rho}_{ij}(\eta, \eta_i, \eta_j, \Delta\phi_{ij}) \right\rangle_{\text{soft-gluon configs.}} \quad (44)$$

over the soft-gluon clouds.

The results shown in Fig. 9 are available in computer-readable form, and through a C++ interface, on request from the authors.

b. Comparing different gluer probes at fixed λ

Eq. (11) is a purely single-logarithmic ($\alpha_s^n \ln^n Q/\mu_{\text{np}}$) result, whereas a shower mixes in subleading logarithms. Here we follow the PanScales approach of examining several α_s values while holding fixed $\lambda = \alpha_s \ln p_{t,\max}/p_{t,\min} = 0.4$, using a fixed coupling for simplicity, and then examining the $\alpha_s \rightarrow 0$ limit. We choose $p_{t,\max} \ll Q$, so as to eliminate subleading effects associated with the limited phase space for hard gluons.

Direct insertion of the gluer according to the generalisation of Eq. (13b) is the most flexible way of probing gluer effects: it can be used with any observable, in both the 2 and 3-jet regions and even with a massive gluer. It is the method we have used in Figs. 4 and 5. Applying it in the 2-jet case yields the orange points of Fig. 10. While the method is flexible, the integration over the gluer kinematics leads to significant Monte Carlo statistical errors. Furthermore, rounding errors make it difficult to probe very small values of $k_{\perp n}/p_{t,\max}$, as needed for both the $\alpha_s \rightarrow 0$ and $k_{\perp n} \rightarrow 0$ limits.

In contrast, the semi-analytic approach, which exploits the fact that the perturbative gluon cloud is uniform in rapidity at single logarithmic accuracy, does not have these limitations. With finite α_s choices, it yields the green points of Fig. 10, which, for each given α_s , are consistent with the orange (gluer insertion) points to within statistical uncertainties. At the largest α_s values, these are well below a percent. The semi-analytic approach can also be run at asymptotically small $\alpha_s = 10^{-9}$ and correspondingly large $\ln p_{t,\max}/p_{t,\min}$ (red dot). The green points' extrapolation, the green line, is consistent with that asymptotic run and with Eq. (11) (blue cross).

Fig. 10 thus validates the asymptotic limit of the semi-analytic method that we used across many λ values in Fig. 3 to confirm Eq. (11). Furthermore, the consistency of the two approaches at finite α_s values, and of the extrapolation with the asymptotic result, helps provide confidence in the interpretation of Figs. 4 and 5, which both relied on finite- α_s studies.

5. Mass schemes

Calculations of non-perturbative power corrections typically use massless partons: indeed, if one has a massive gluer as an intermediate step, a typical full calculation will account for the decay of that massive gluer, according to the well-known double-soft matrix element, which leads to the Milan factor [20–23], a pure number that multiplies the result obtained with a single massless parton. The Milan factor is universal across linear observables.

In practice, however, experiments measure massive hadrons. It has long been understood that different definitions of an event shape observable, for example the choice to use the modulus of a 3-vector or an energy, will lead to Λ/Q non-perturbative corrections that differ [57] (see also [58]). What's more, the difference between various mass schemes appears to come with its own anomalous dimension, which differs from that calculated here for massless gluer emission. A question that naturally arises is whether there is an “ultimate” scheme for the treatment of massive hadrons for which the relevant anomalous dimension is just that calculated in this letter.

First, let us recall the main schemes for treating hadron masses, and which might be good candidates for the ultimate scheme.

- *P*-scheme: every particle i is replaced with a massless particle with E_i set equal to $|\vec{p}_i|$; the centre of mass energy in the normalisation of the event shape is calculated from the sum of all the updated particle momenta. Ref. [57] found that this scheme breaks the c_V scaling of the non-perturbative coefficient for different event shapes as calculated with a massless gluer, e.g. the ratio of the C -parameter and thrust non-perturbative corrections is no longer $3\pi/2$. Even though the breaking is numerically small in practice (the exact breaking depends on the distribution of m/k_t for the hadrons), that suggests that this scheme may be disfavoured.
- *E*-scheme: every particle i is replaced with a massless particle, with \vec{p}_i multiplied by $E_i/|\vec{p}_i|$. In the original event's centre of mass frame, the sum of 3-momenta may no longer add up to zero, and so the event is boosted back into the centre-of-mass frame. Ref. [57] found that this preserves the c_V scaling found in the massless calculation, independently of the distribution of m/k_t , and so is a good candidate scheme.
- *D*-scheme: every massive particle is replaced by two massless particles, corresponding to an effective 2-body decay for all massive particles. This scheme too preserves the c_V scaling found in the massless calculation and so appears to be as good a candidate as the *E*-scheme.

Besides the question of the scaling of the c_V , there are some general principles that strongly favour the *D*-scheme: the conservation of momentum in the decay implies that the relation between transverse and $+/ -$ light-cone components along any given dipole's two directions will be preserved. As discussed in §3, this is one of the elements that is relevant to the all-order exponentiation of the anomalous dimension. Viewed another way, for asymptotically soft gluers, the insertion of a single massive gluer that then decays gives identical kinematics for the $q\bar{q}$ system as compared to the sequential insertion of two massless gluers with the same kinematics as the gluer decay products. Conversely, the *E* and *P* schemes both effectively introduce a global element to the redistribution of longitudinal momentum with respect to any given dipole direction, and so one might expect that they will not reproduce various properties that we rely on for the derivations in the massless case.

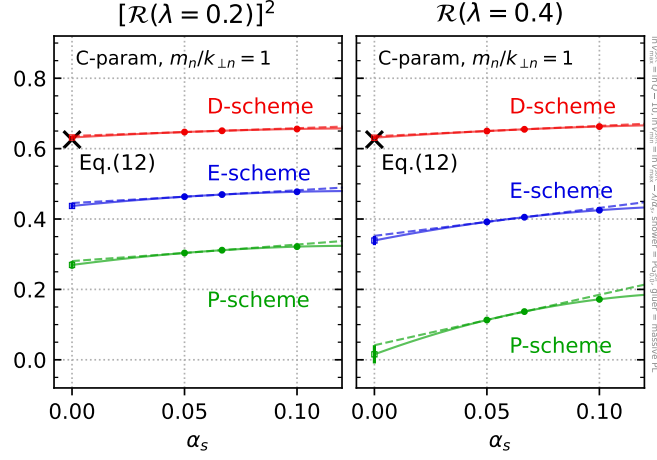


FIG. 11. Calculation of \mathcal{R} with massive gluon insertion in 3 schemes for the treatment of hadron masses, shown as a function of different finite α_s values, together with the extrapolation for $\alpha_s \rightarrow 0$. Left: $[\mathcal{R}(\lambda = 0.2)]^2$, right $\mathcal{R}(\lambda = 0.4)$. The plot embodies two tests: whether the $\alpha_s \rightarrow 0$ extrapolation (point at $\alpha_s = 0$) agrees with the massless calculation (black cross); and, if it doesn't, whether it still exponentiates, in which case the extrapolations would agree with between the two panels. The solid lines show quadratic extrapolations based on all three α_s points, while the dashed lines show a linear extrapolation based on the two smallest α_s points. The plot thus confirms that the D -scheme gives results that are consistent with the massless calculation, while the E and P -schemes do not, and furthermore do not exponentiate.

To explore this question in greater depth, we considered an explicit kinematic map for insertion of a massive gluon. For a dipole of mass M , consisting of particles with massless momenta \tilde{p}_i and \tilde{p}_j , and a non-perturbative gluon of transverse momentum $k_{\perp n}$ and mass m_n , the map is

$$k_n^\mu = z_+ \tilde{p}_i^\mu + z_- \tilde{p}_j^\mu + k_{\perp n}^\mu, \quad (45a)$$

$$p_i^\mu = (1 - z_+) \tilde{p}_i^\mu + \frac{k_{\perp n}^2}{M^2(1 - z_+)} \tilde{p}_j^\mu - k_{\perp n}^\mu, \quad (45b)$$

$$p_j^\mu = \left(1 - z_- - \frac{k_{\perp n}^2}{M^2(1 - z_+)}\right) \tilde{p}_j^\mu, \quad (45c)$$

with

$$z_+ = \sqrt{k_{\perp n}^2 + m_n^2} \sqrt{\frac{\tilde{s}_j}{\tilde{s}_{ij}\tilde{s}_i}} e^{\bar{\eta}}, \quad z_- = \sqrt{k_{\perp n}^2 + m_n^2} \sqrt{\frac{\tilde{s}_i}{\tilde{s}_{ij}\tilde{s}_j}} e^{-\bar{\eta}}. \quad (46)$$

With this map for the massive gluon insertion, we can then investigate how all-order rescaling factor \mathcal{R} of Eq. (11), when extended to massive gluons, depends on the ratio of the gluon mass m_n to its transverse momentum $k_{\perp n}$. We evaluate the rescaling factor \mathcal{R} for the non-perturbative gluon effect, evaluated using the same structure of soft-gluon cloud as used in the $\alpha_s = 0.1$ points of Fig. 10. Specifically, we start from a $q\bar{q}$ event and add a perturbative soft-gluon cloud with transverse momenta p_t in the range $10 < \ln Q/p_t < 10 + \lambda/\alpha_s$. We then probe how the C -parameter changes on inserting a massive gluon, as compared to the integrated gluon effect in a pure $q\bar{q}$ event without the soft-gluon cloud. That gives us \mathcal{R} .

Fig. 5 of the main text shows \mathcal{R} for several values of $m_n/k_{\perp n}$, in each of the three mass schemes. Clearly for $m_n/k_{\perp n} = 0$, all schemes must agree with the result in Fig. 10 at the corresponding α_s value, and one sees that they do. For the E and P schemes, the anomalous scaling factor \mathcal{R} depends on $m_n/k_{\perp n}$. Assuming this same pattern carries through to massive hadrons, this would prevent us from predicting linear power corrections in terms of a single $T_{q\bar{q}}$ parameter, since we would also need to know the distribution of m/k_{\perp} for the hadrons in order to determine the rescaling factor \mathcal{R} at any given λ . In contrast, in the D scheme, the rescaling factor \mathcal{R} is independent of the gluon mass, suggesting that the simple form Eq. (11) should hold independently of the distribution of hadron masses, and that the Λ/Q hadronisation corrections can be represented in terms of a single non-perturbative parameter, i.e. a single effective $T_{q\bar{q}}$.

Fig. 11 shows a further study. The left and right-hand panels display \mathcal{R} for the C -parameter for each of two values of $\lambda = \{0.2, 0.4\}$, now with a fixed $m_n/k_{\perp n} = 1$, and plotted as a function of α_s so that one can explore the $\alpha_s \rightarrow 0$

limit. The right-hand panel, for $\lambda = 0.4$, can be directly compared to the massless gluer calculation of Fig. 10. If the anomalous scaling exponentiates, the left-hand panel, showing \mathcal{R}^2 for $\lambda = 0.2$, should show an effect that is identical to the right-hand panel. As anticipated on general grounds, and as expected already from Fig. 5, the D -scheme results are consistent with the massless limit and, so, with exponentiation in the $\alpha_s \rightarrow 0$ limit. In contrast, the E -scheme and P -scheme clearly do not satisfy exponentiation and they show significantly stronger anomalous scaling than the D -scheme results, as was already seen in Fig. 5.

6. Continuous bin edges for energy correlators

In our studies of gluer insertion for the EEC with a condition $|\cos\theta| < 1/2$, we found that at large Q values and very small $k_{\perp n}$, there were large statistical uncertainties. These appear to be associated with situations where a perturbative gluon (with transverse momentum p_t) is close to the θ boundary, within an angle of order $k_{\perp n}/p_t$. A gluer with a large z_+ light-cone momentum fraction can go to the other side of the boundary, changing the observable by an amount that can be almost as large as $p_t/Q \gg k_{\perp n}/Q$. Ultimately such effects average out to be small: sometimes the perturbative gluon is outside the boundary and sometimes it is inside, changing the sign of the effect, and the effect is only present in the rare situations where the perturbative gluon is close to the boundary. Nevertheless the effect leaves a large trace in the dispersion of the result.

To work around this issue, we found it useful to adopt a continuous bin, in analogy with Eq. (38)

$$\text{EEC}(|\cos\theta| \lesssim 1/2) = \sum_{i,j} \frac{E_i E_j}{Q^2} f(|\cos\theta|) \quad f(c) = \Theta(0.4 < c < 0.6) \times \left(\frac{0.6 - c}{0.2} \right) + \Theta(c < 0.4). \quad (47)$$

This greatly reduced the statistical fluctuations. It is our understanding that such continuous bins are sometimes used also to improve the stability of fixed-order perturbative calculations, though this point is not necessarily always explicitly discussed.

7. Study of Q dependence of shifts in distributions

Fig. 12 shows versions of Fig. 6 for a wide range of Q values, $Q = \{30, 91.2, 1000, 10000\}$ GeV and for both the C -parameter (left) and the thrust (right). Starting with the C -parameter, one sees that as Q is increased above 91.2 GeV, there is quite remarkable agreement between three different sets of the results: the analytic $\mathcal{R}(\mu)$ rescaling, the direct gluer insertion into the shower, and Pythia. Instead, at the lowest Q value of 30 GeV, the uncertainties associated with the insertion scale and map for the gluer (red band) grow significant. Those uncertainties are important in terms of obtaining consistency with Pythia's hadronisation correction.

For the thrust, two main remarks are in order: the uncertainty associated with the insertion scale and map for the gluer (red band) is more substantial than for the C -parameter, for reasons that we have yet to elucidate. Furthermore the difference between the rescaled 3-parton result (dark blue) and the gluer insertion (dark red) remains significant even at very high Q values. This difference is a potential measure of further higher-order effects. Given that the leading-order thrust distribution goes to zero linearly at $\tau = \frac{1}{3}$, the fractional NLO correction to the distribution there diverges as $1/(\tau - \frac{1}{3})$, and one might therefore expect the thrust to be less perturbatively stable than the C -parameter, where such a power divergence does not occur. However we have not been able to translate this observation into a more quantitative expectation for the difference between the two approaches. Nevertheless, overall, Fig. 12 suggests that the thrust is a less stable observable than the C -parameter when it comes to estimating non-perturbative corrections, a consideration that should probably be taken into account in strong-coupling determinations.

A final comment concerns the choice of μ in the $\mathcal{R}(\mu)$ rescaling of the 3-parton result. For a single soft gluon at zero rapidity, the transverse momentum of the gluon is given by $p_t = CQ/3$ or $p_t = \tau/Q$. As a default choice for μ we take this p_t divided by 1.5, on the grounds that the soft resummation will start somewhere below the actual hardest gluon. We choose an uncertainty band such that μ does not exceed this p_t .

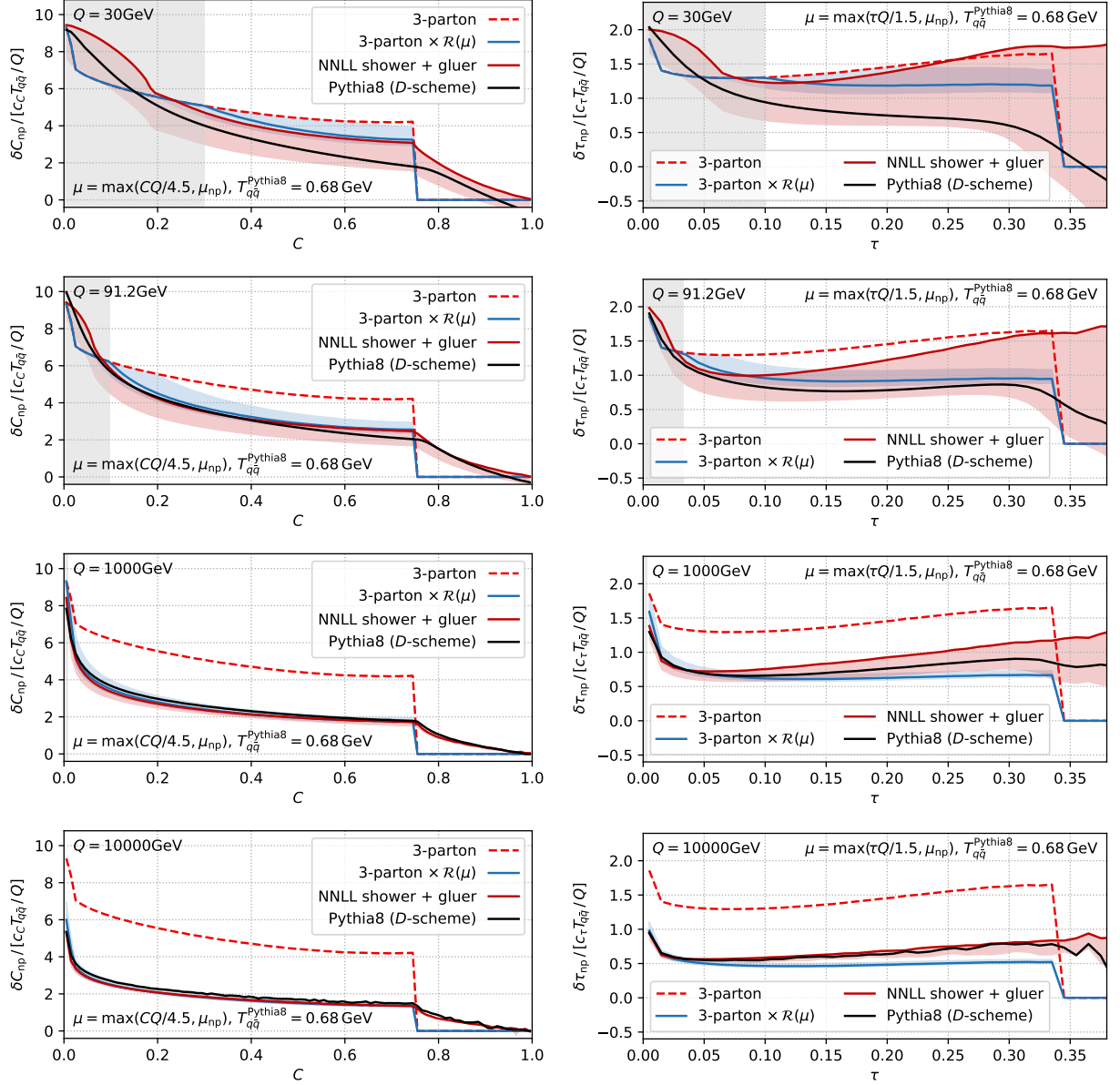


FIG. 12. Non-perturbative shifts in the C -parameter (left) and thrust (right) for multiple values of the centre-of-mass energy Q . The set of curves is the same as in Fig. 6. Specifically, the dark red line corresponds to gluer insertion into a shower that runs down to a scale $\mu_{np} = 2$ GeV. That insertion is carried out with the PL shower and a scale $k_{\perp n} \simeq 0.0015$ GeV, while the red band shows the uncertainty when the insertion switches to $k_{\perp n} \simeq 0.7$ GeV with the PG shower. For the dark blue line, based on Eq. (11), the band shows the impact of varying μ by a factor of 1.5 up (2 down) around the central choice as shown in the figure. The motivation for the central scale choice is shown discussed in the text. As was the case in Fig. 6, the grey area indicates $CQ/4.5 < \mu_{np} = 2$ GeV, where we freeze μ to μ_{np} and where the perturbative shower cutoff in the gluer insertion curve starts to have an effect.